Available online at www.sciencedirect.com
SCIENCE DIRECT®
Polymer 44 (2003) 4589–4597
polymer
www.elsevier.com/locate/polymer

Time dependent deformation behavior of thermoplastic elastomers

H.H. Le[a], Th. Lüpke[a], T. Pham[b], H.-J. Radusch[a,*]

[a]*Polymer Engineering, Institute of Materials Science, Martin Luther University Halle Wittenberg D-06099 Halle (Saale), Germany*
[b]*Borealis GmbH, Linz, Austria*

Received 20 January 2003; received in revised form 9 May 2003; accepted 12 May 2003

Abstract

The analysis of the stress relaxation behavior of thermoplastic elastomers (TPE) was made with the help of the two-components model, which allows a consistent description of the time and temperature dependent behavior. The effect of draw ratio, strain rate and temperature on the stress relaxation behavior of TPE was investigated. The structural background of the relaxation behavior was discussed using the two-network model shown in form of an analogy model. The assignation of the stress components to a hard phase and soft phase network is based on the experimental results taking into consideration the knowledge about the structural nature and deformation performance of TPE. Comparing dynamic vulcanizates with different TPE based on block copolymer, it was found that the characteristic differences in the time-dependent deformation behavior of the different TPE are based on the different deformation behavior of the network points.

Keywords: Thermoplastic elastomers; Stress relaxation; Deformation behavior

1. Introduction

After pioneering work of Coran and Patel [1] dynamic vulcanizates have been successfully introduced into the market of thermoplastic elastomers (TPE). With their special morphology consisting of cross-linked rubber particles finely distributed in a thermoplastic matrix these materials exhibit good elastomeric properties at room temperature. At elevated temperatures however, they melt like thermoplastics, so that they are ready for highly productive thermoplastic processing techniques. The preparation of dynamic vulcanizates by combining commercially available rubber and thermoplastic components enables a wide spectrum of properties and applications. This is the motivation for the intensive investigation on structure formation, deformation mechanism [2–5], compatibilization [6], process and recipe optimization [7] and medial behavior [8].

Compared to vulcanized rubber the properties of dynamic vulcanizates are influenced by the thermoplastic nature of the material. This results in a considerable dependence of the mechanical properties on time and temperature. Thus, for confident application of these materials a detailed knowledge about their viscoelastic behavior, especially the long-term performance, is required. However, it has been insufficiently studied so far [9–11].

In our investigation we used the stress relaxation technique to characterize the long-term behavior of TPE [5]. The goal of the present work is to study the effect of the test conditions like draw ratio, loading rate and temperature on the stress relaxation behavior. Additionally, the correlation between the time dependent deformation behavior and the structural features of TPE was established in order to control the mechanical behavior by optimization of the mixture.

1.1. Theoretical background

In a stress relaxation experiment the sample is loaded to a defined deformation. Keeping this deformation constant, the stress decay is recorded in dependence on time. As schematically shown in Fig. 1 the stress relaxes to a steady state value, which is usually higher than zero.

To evaluate the relaxation curve, the applied stress σ is separated into two components, a relaxing stress component

* Corresponding author. Tel.: +49-3461-462-791; fax: +49-3461-46-38-91.
E-mail address: hans-joachim.radusch@iw.uni-halle.de (H.J. Radusch).

0032-3861/03/$ - see front matter © 2003 Elsevier Science Ltd. All rights reserved.
doi:10.1016/S0032-3861(03)00409-9

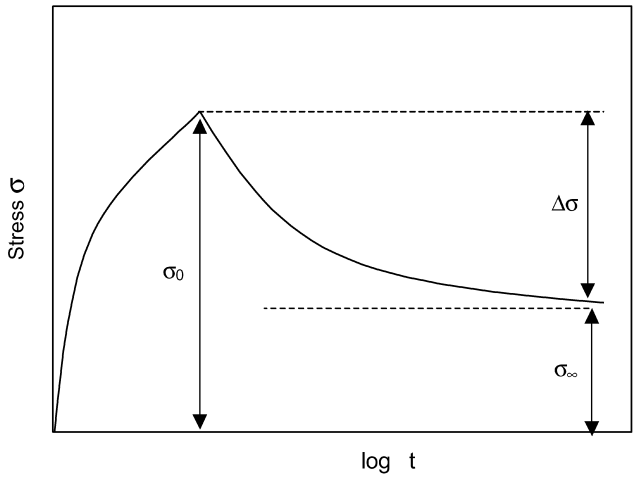

Fig. 1. Stress relaxation experiment and the two stress components σ_∞ and $\Delta\sigma$.

$\Delta\sigma$ and a non-relaxing stress component σ_∞ :

$$\sigma(t) = \Delta\sigma(t) + \sigma_\infty \tag{1}$$

According to Seeger [12,13] the relaxing stress component $\Delta\sigma(t)$ is called thermal stress component, because it acts on short-range obstacles, which can be overcome by stress aided thermal activation. It depends on the plastic deformation rate $\dot{\varepsilon}$ and the temperature T according to Eyring's rate theory [14]:

$$\Delta\sigma = \frac{\Delta H}{v} - \frac{kT}{v}\ln\frac{\dot{\varepsilon}_0}{\dot{\varepsilon}} \tag{2}$$

In contrast to the relaxing stress component, the non-relaxing stress component σ_∞ is called athermal stress component. It is originated from long-range stress fields, which cannot be overcome by the thermal activation.

The separation of the applied stress into two components according to Eq. (1) can be characterized by a simple parallel model, which is often used to describe the viscoelastic behavior of polymers. Ferry [15] introduced, for example, into his two-component model (TC model) a relaxation time function $\Phi(t)$ to describe the time dependence of the relaxation processes: $\sigma(t) = \sigma_\infty + \Delta\sigma(t) = \sigma_\infty + \Delta\sigma_0\Phi(t)\Delta\sigma_0$ is the relaxing stress component at the beginning of the relaxation process. The relaxation time function $\Phi(t)$ forms a strictly symmetrical S-shaped curve on the log time scale. It drops from unity to zero. As a special feature of the TC model the relaxation time function $\Phi(t)$ is found to be independent of the temperature. For a wide variety of materials [9,16,17] it shows a universal shape [18–23].

Because of the invariance of the shape of the relaxation time function $\Phi(t)$, only three parameters are necessary to describe the relaxation curve: the relaxation time τ which characterizes the position of the curve on the logarithmic time scale and the stress components σ_∞ and $\Delta\sigma$.

2. Experimental

2.1. Materials and sample preparation

For the experimental investigation dynamic vulcanizates of polypropylene (PP) and nitrile rubber (NBR) have been prepared in laboratory scale. The dynamic vulcanization was carried out in a double-rotor static lab mixer (Brabender Plasticoder PL-2100) with a mixing temperature of 170 °C. Polypropylene PP (Daplen KFC 2008, Borealis) and Acrylnitril-Butadiene-Rubber NBR (Nippol DN-401LL, Zeon Germany) were used as thermoplastic and elastomeric components, respectively. Phenolic resin (PA 510, Vianova Resins) acted as cross-linking agent. The mixture composition as well as the amount of the cross-linking agent were varied systematically. After removing from the mixer dynamic vulcanizates were compression molded at 210 °C to get thin sheets of 200 μm thickness. Samples of about $15 \times 3 \times 0.2$ mm were cut from these sheets for further mechanical investigation.

In order to compare the mechanical behavior of dynamic vulcanizates with other commercial TPE, following products were used: elastic polypropylene (ePP) (Reflex 201w, Borealis), poly (ether-block-amide) PEBAX (PEBAX 3533, Elf Atochem) and styrol-ethylene-butadiene-styrol triblock copolymer SEBS (Kraton FG 1901X, Shell Chemical). For the investigation of the hard phase in TPE, the following corresponding thermoplastics were used: isotactic polypropylen PP (Daplen KFC 2008, Borealis), polystyrol PS (polystyrol 143 E, BASF) and polyamide PA 12 (Grilamid L25, EMS-Chemie).

2.2. The relaxation experiment

Stress relaxation experiments were performed using a dynamic mechanical analyser DMTA 3e (Rheometric Scientific) in the tensile mode. The instrument is equipped with a temperature chamber, which enables a long-term constancy of the temperature (deviation <0.1 K).

Relaxation experiments were executed after loading by different strain rates $\dot{\varepsilon}$ ($1 \times 10^{-4}\mathrm{s}^{-1}$ $\dot{\varepsilon} < 1.7 \times 10^{-1}s^{-1}$) to different draw ratios λ ($1.05 < \lambda < 4.5$) at different temperatures T (-20 °C $< T <$ 130 °C).

All relaxation curves were recorded over a period of about 15 h with a maximum resolution of 0.1 s. No steady state stress value had been observed after 15 h. Therefore, extrapolation procedures have been applied to determine the non-relaxing stress component σ_∞. In our case we used an extrapolation method proposed by Li [24].

3. Results

3.1. Effect of loading rate

In the ideal case, the stress relaxation has to be measured

after a stepwise loading of the sample. Practically however, a defined time period is necessary to reach the final draw ratio. Relaxation processes during loading influence the stress relaxation behavior. This behavior is shown in Fig. 2(a) comparing the stress relaxation curves of dynamic vulcanizates, loaded at different strain rates $\dot{\varepsilon}$ to a predetermined deformation ratio $\lambda = 2$. Reduced strain rate increases the time to reach the final draw ratio and reduces the stress σ_0 at the beginning of the stress relaxation process. The influence of loading rate on the stress relaxation curves is limited to the short time scale. After longer relaxation times the effects of loading rate are negligible on the logarithmic time scale. To eliminate the influence of the loading rate a horizontal shift of the stress relaxation curves on the time axis by a strain rate dependent value c was applied. Assuming c to be the reciprocal of the strain rate $\dot{\varepsilon}$, a strain-rate independent master curve results as shown in Fig. 2(b). Deviations of the experimental data from the master curve at the beginning of the relaxation experiment were attributed to the limited accuracy of time measurement.

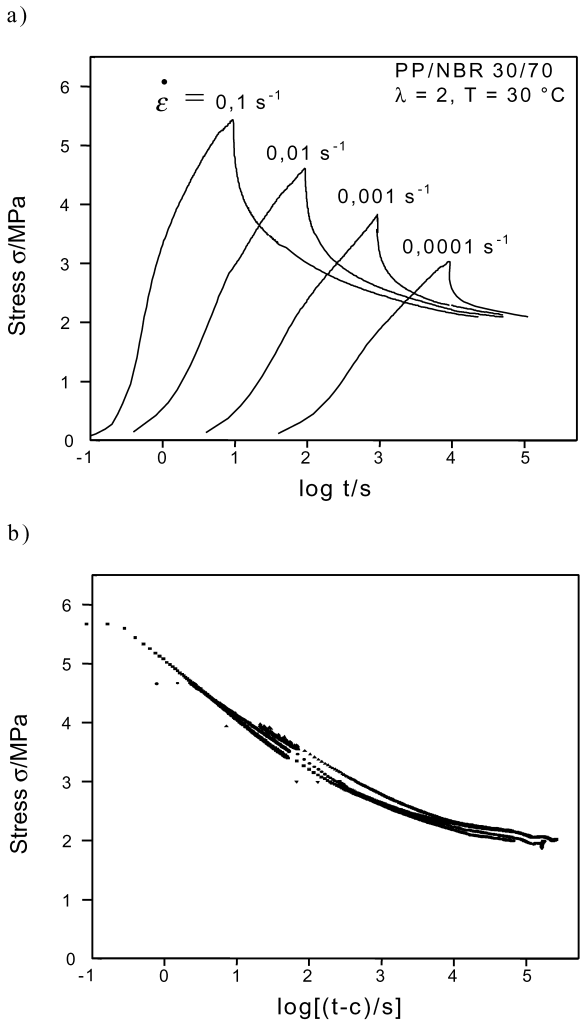

Fig. 2. (a) Stress relaxation of dynamic vulcanizate PP/NBR 30/70 at different strain rates $\dot{\varepsilon}$ (b) master curve created by horizontal shifting of the relaxation curves.

From the stress relaxation curves in Fig. 2(b) the thermal and athermal stress components $\Delta\sigma$ and σ_∞ were calculated and plotted in Fig. 3 as a function of the strain rate. According to its athermal character the non-relaxing stress component σ_∞ is not affected by the strain rate. On the other hand, the relaxing component $\Delta\sigma$ increases linearly with the logarithm of the strain rate $\dot{\varepsilon}$. From the slope of the straight line of $\Delta\sigma$ in Fig. 3, the activation volume v can be calculated using Eyring's Eq. (4):

$$v = kT \frac{\mathrm{d} \ln \dot{\varepsilon}}{\mathrm{d}\, \Delta\sigma} \tag{4}$$

From Eq. (4) an activation volume of about 5 nm^3 was determined with respect to the thermoplastic content ϕ. A similar result was obtained by Liu and Truss [25] using a more precise two-stage model. They found that for pure PP the activation volume was approximately 4 nm^3. It corresponds to a volume of about 10 monomer units of propylene.

3.2. Effect of the draw ratio

Many works have been done to characterize the stress relaxation behavior of polymers in the linear range at the draw ratios λ of less than about $\lambda = 1.01$ [18–23]. In this range, the stress relaxation modulus $E(t)$ does not depend on the deformation. However, rubbery materials like TPE are usually applied at draw ratios far above the linear viscoelastic limit. Thus, the influence of deformation on stress relaxation behavior deserves special attention.

To investigate the contribution of the draw ratio, stress relaxation experiments had been performed at different draw ratios between $\lambda = 1.05$ and 4.5. Test temperature $T = 30\,^{\circ}\mathrm{C}$ and loading rate $\dot{\varepsilon} = 0.17\ \mathrm{s}^{-1}$ were kept constantly. The resulting relaxation curves are given in a double logarithmic scale in Fig. 4(a).

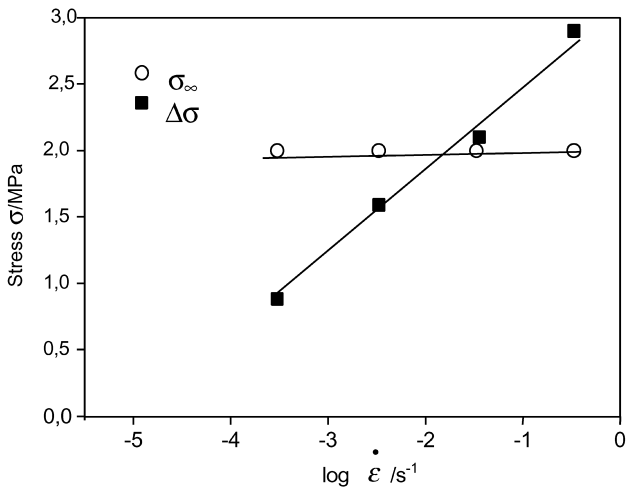

Fig. 3. Dependence of stress components σ_∞ and $\Delta\sigma$ on strain rate $\dot{\varepsilon}$.

With increasing draw ratio, the relaxation curves are shifted to higher stress. However, the shape of the curves remains unchanged in the double logarithmic plot. So it is possible to superimpose the relaxation curves by a vertical shift. The shift procedure can be described by a simple nonlinear viscoelastic approach according to Eq. (5) and (5a), respectively.

$$\sigma(t,\lambda) = f(\lambda)E(t) \tag{5}$$

$$\log \sigma(t,\lambda) = \log f(\lambda) + \log E(t) \tag{5a}$$

Based on Eq. (5a), the subtraction of the logarithm of the deformation function $f(\lambda)$ from the logarithm of the stress $\sigma(t,\lambda)$ results in a single master curve, which characterizes the time dependent modulus $\log E(t)$. This master curve is not affected by the draw ratio. Therefore, it characterizes a

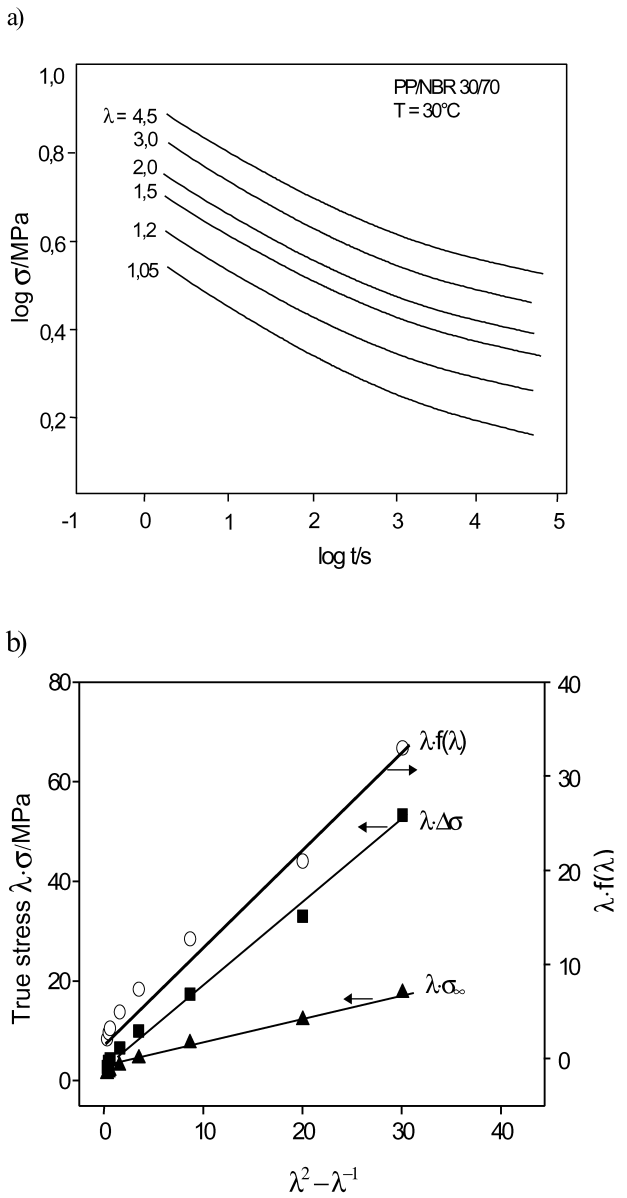

Fig. 4. (a) Stress relaxation of dynamic vulcanizate PP/NBR 30/70 at different deformation λ (b) deformation dependence of stress components.

'quasi-linear' viscoelastic behavior, which has already been reported for PP [17–23], HDPE [26] and for several amorphous polymers [27].

Eq. (6), resulting from the simple rubber elasticity theory, was used to describe the influence of deformation on relaxing and non-relaxing stress components.

$$\sigma^t = (\lambda^2 - \lambda^{-1})E^R = (\lambda^2 - \lambda^{-1})\frac{3\rho kT}{\bar{M}_w} \tag{6}$$

In Eq. (6) σ^t denotes the true stress, e.g. the applied force with respect to the actual cross section of the specimen. The rubber elastic modulus E^R depends on the density ρ, the Boltzmann constant k, the absolute temperature T and the average molecular weight between cross-links $\bar{M}_w$.

True values of the thermal and athermal stress components were calculated as a product of the engineering stresses $\Delta\sigma$ and σ_∞ and the draw ratio λ. For this calculation, a constant volume during deformation was assumed. The plot of $\lambda\Delta\sigma$ and $\lambda\sigma_\infty$ against the rubber elastic deformation function $(\lambda^2 - \lambda^{-1})$ in Fig. 4(b) gives straight lines for both stress components indicating the existence of two different network structures in the material. A detailed analysis of the character of the deformation function $f(\lambda)$ by comparing Eqs. (4) and (6) shows, that it corresponds to $(\lambda - \lambda^{-2})$. Accordingly, the plot of $\lambda f(\lambda)$ against $(\lambda^2 - \lambda^{-1})$ in Fig. 4(b) gives a straight line with a slope of about 1.

An average molecular weight between the cross-links of about $\bar{M}_w = 3000$ g/mol was calculated from the slope of the non-relaxing stress component σ_∞. This corresponds to the values determined on dynamic vulcanizates of PP and EPDM rubber by swelling experiments [28] and characterizes the permanent network with stable cross-links independent on time. Besides this permanent network, a second network exists with time dependent cross-links. This network determines the deformation dependence of the relaxing stress component $\Delta\sigma$.

3.3. Effect of temperature

Temperature is an important factor determining the molecular mobility of the material. An increase in the temperature accelerates thermally activated processes and reduces relaxation times. This behavior is shown in Fig. 5(a) by the stress relaxation curves which have been measured at temperatures between −20 and 130 °C. Increased temperature shifts the relaxation curves horizontally to shorter times and at the same time vertically to lower stresses. The horizontal shift causes a decrease of the thermal stress component $\Delta\sigma$. The vertical shift of relaxation curves causes a linear decrease of the athermal stress component σ_∞.

Thermal and athermal stress components determined from the relaxation curves shown in Fig. 5(a) are plotted in dependence on the temperature in Fig. 5(b). The thermal stress component attributed to thermally activated processes

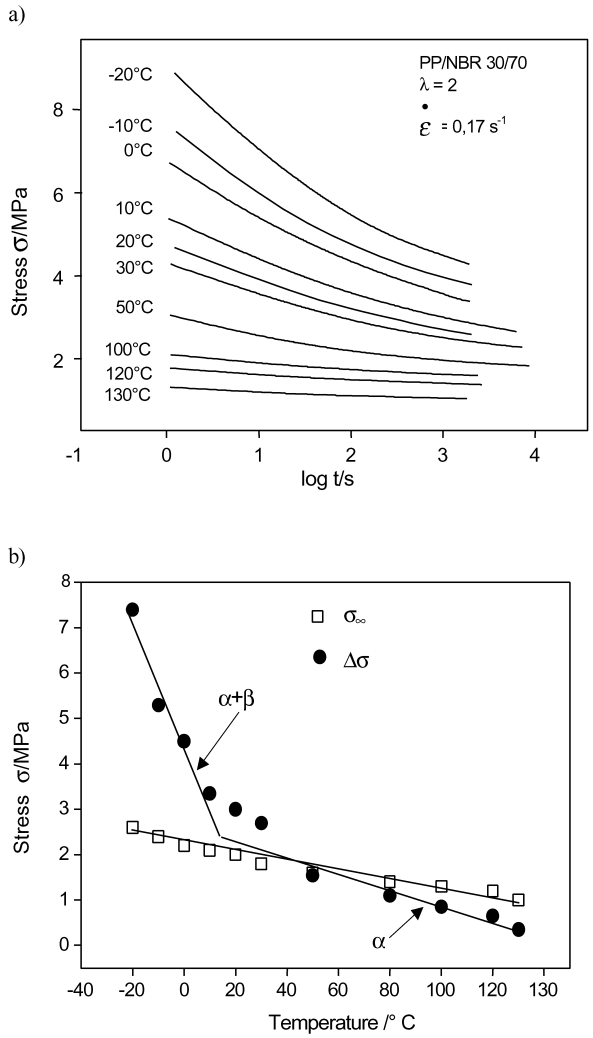

Fig. 5. Stress relaxation at different temperatures and temperature dependence of stress components.

is characterized by a non-linear curvature, which can be approximated by two straight lines. This is an indication of different relaxation processes taking place in the temperature range investigated. It is assumed that the intersection point at about 10 °C corresponds to the glass transition temperature of the PP matrix. Based on the Eyring's Eq. (2) the activation energy E_A can be calculated from the temperature dependence of the relaxing stress component:

$$\frac{d\,\Delta\sigma}{dT} = -\frac{E_A}{vT} \tag{7}$$

Using Eq. (7) with a PP content $\phi = 0.3$ and an activation volume $v = 5\,\mathrm{nm}^3$ an activation energy E_A of about 98 kJ mol^{-1} was calculated at temperatures above 10 °C. This activation energy is close to the activation energy of the α-process of crystalline PP phase measured in this temperature range by dynamic mechanical analyses ($E_A^{DMA} = 132$ kJ mol^{-1}) and to the corresponding results from literature (107–150 kJ mol^{-1}) [29]. At temperatures below 10 °C the glass transition of the amorphous phase of the PP matrix influences the relaxation behavior so that the viscoelastic component $\Delta\sigma$ increases strongly.

In contrast to Seeger's theory the athermal stress component also depends on temperature. However, the linear behavior over the whole investigated temperature range investigated indicates, that short-range relaxation processes do not influence the athermal stress component. Thus, it can be assumed, that the temperature dependence of the athermal stress component is triggered by the temperature dependent structural changes [30,31].

Because of the temperature dependence of the athermal stress component the rheological behavior of the dynamic vulcanizates is very complicated. Therefore, the master curve construction from the experimental stress relaxation curves is not possible by a simple horizontal shift. To create a master curve in this case, the horizontal shift has to be applied only to the relaxing stress component. The temperature dependence of the athermal stress component acts as a vertical shift factor. For a reference temperature T_R the stress relaxation master curve could be calculated as follows:

$$\sigma(t,T) = [\sigma_\infty(T) - \sigma_\infty(T_R)] + \Delta\sigma(t/a_T) \tag{8}$$

The master curve for a reference temperature of 30 °C determined from the experimental results is shown in Fig. 6. A very good fit is observed for the experimental data determined at temperatures above 10 °C since only the α-process of PP controls the relaxation behavior. With the experimental data measured at temperatures below 10 °C, where α and and β processes are operating simultaneously, a correct master curve construction is not possible.

In Fig. 7(a) and (b) the temperature dependence of the horizontal and vertical shift factors are shown. The temperature dependence of the horizontal shift factors a_T follows the Arrhenius approach. The Arrhenius diagram (Fig. 7(a)) gives a straight line at temperatures between 10 and 130 °C. From the slope of the line an activation energy of $E_A = 110$ kJ mol^{-1} was calculated. It is consistent with the activation energy calculated from the time and

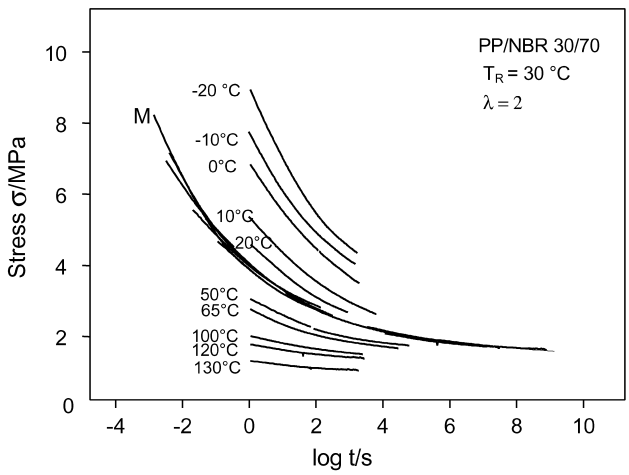

Fig. 6. Master curve of dynamic vulcanizate PP/NBR 30/70.

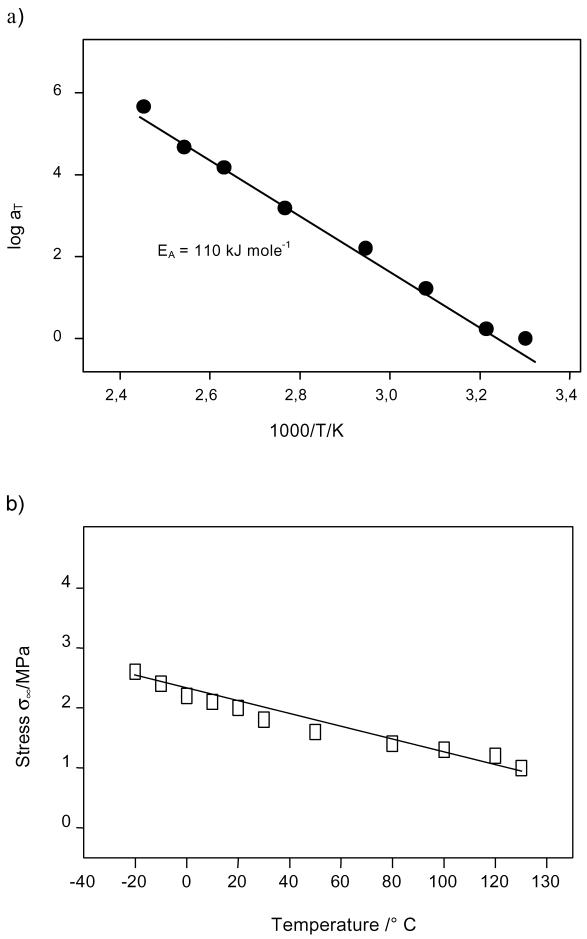

Fig. 7. Temperature dependence of the horizontal and vertical shift factor.

temperature dependence of the relaxing stress component using Eyring's Eq. (7). This finding indicates that both effects are originated from the same molecular mechanisms. In the Fig. 7(b) the temperature dependence of the athermal stress component is shown. In this case, this dependence represents the vertical shift factor. The larger the slope, the more strongly the relaxation curve shifts vertically to lower stress by increasing temperature.

The influence of the temperature on the stress relaxation behavior was described by two quantities: the activation energy E_A and the athermal stress component σ_∞. They are characteristic for two different temperature-dependent processes, i.e. for viscoelastic processes and temperature-dependent structural changes.

3.4. Effect of the composition

Mixture composition such as thermoplastic content ϕ and amount of cross-linking agent υ has a characteristic influence on the stress relaxation behavior of dynamic vulcanizates. Based on the athermal stress component σ_∞ and the activation energy E_A the influence of thermoplastic content and amount of cross-linking agent has been discussed. In Fig. 8(a) the temperature dependence of the athermal stress component is shown for dynamic vulcanizates of various thermoplastic contents. The thermoplastic content influences the slope of the straight lines. The larger the thermoplastic content, the steeper the slope, and the more strongly the stress relaxation curve shifts vertically downward.

The effect of the amount of vulcanizing agent υ on the temperature dependence of the athermal stress component is demonstrated in Fig. 8(b). An increasing amount of cross-linking agent only changes the position of the straight lines, but not the slope. That means that the vertical shift of the relaxation curves by increasing temperature does not depend on the amount of cross-linking agent or on the modification of the soft phase.

Fig. 9 shows that the activation energies of dynamic vulcanizates and of PP are in the same order of magnitude and are not affected by the blend composition. That means that by increasing temperature the relaxation curve of dynamic vulcanizates shifts horizontally to shorter times as strongly as PP. The PP phase is responsible for the viscoelastic deformation processes in dynamic vulcanizates.

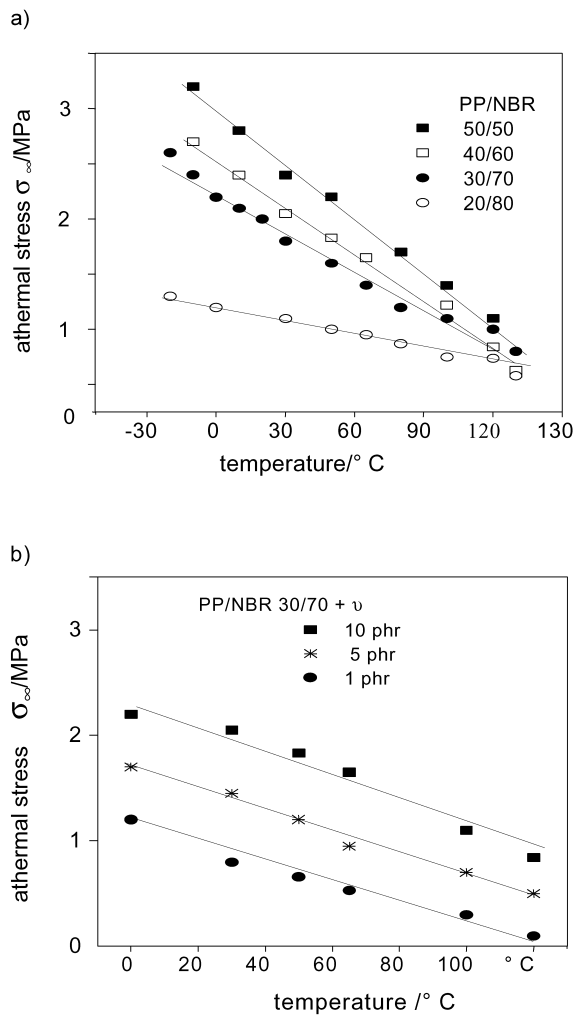

Fig. 8. Temperature dependence of athermal stress components by different thermoplastic content ϕ and amount of cross-linking agent υ.

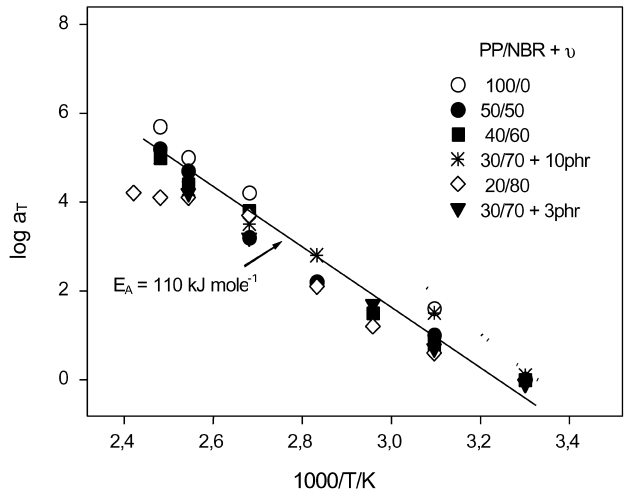

Fig. 9. Temperature dependence of horizontal shift factor by different blend compositions.

Based on the experimental results, the relaxation mechanisms can be assigned to the structure units of dynamic vulcanizates. The TEM micrograph shows a typical morphology of a dynamic vulcanizate with rubber particles dispersed in the thermoplastic matrix (Fig. 10(b)). Two networks co-exist in this morphology according to the two-network model (10d). The soft phase network consists of the elastomeric phase with chemical network points and the amorphous PP phase with entanglements. The hard phase network is built up by the crystalline PP lamella. According to the experimental results, in the application temperature range only the hard phase network is responsible for the time and temperature dependence of the deformation behavior. The hard phase network is schematically shown in Fig. 11, apart from a network of the conventional vulcanizate. The chemical network points of the conventional vulcanizates are time and temperature stable. In the vulcanizates the dominating deformation behavior is rubber elastic. In contrast to that, the chain sliding processes in PP lamellas of the hard phase network cause a thermal stress component $\Delta\sigma$ depending on time and temperature.

The athermal stress component σ_∞ is required to overcome the long-range obstacles made by the net points [12,13]. The value of σ_∞ depends on the rubber elastic behavior of the network on the one hand and on the plastic deformation of the crystalline domains, on the other hand. Thus, the stress relaxation behavior of dynamic vulcanizates is controlled not only by the viscoelastic behavior. It is a summarized result of viscoelastic, elastic and plastic deformation processes.

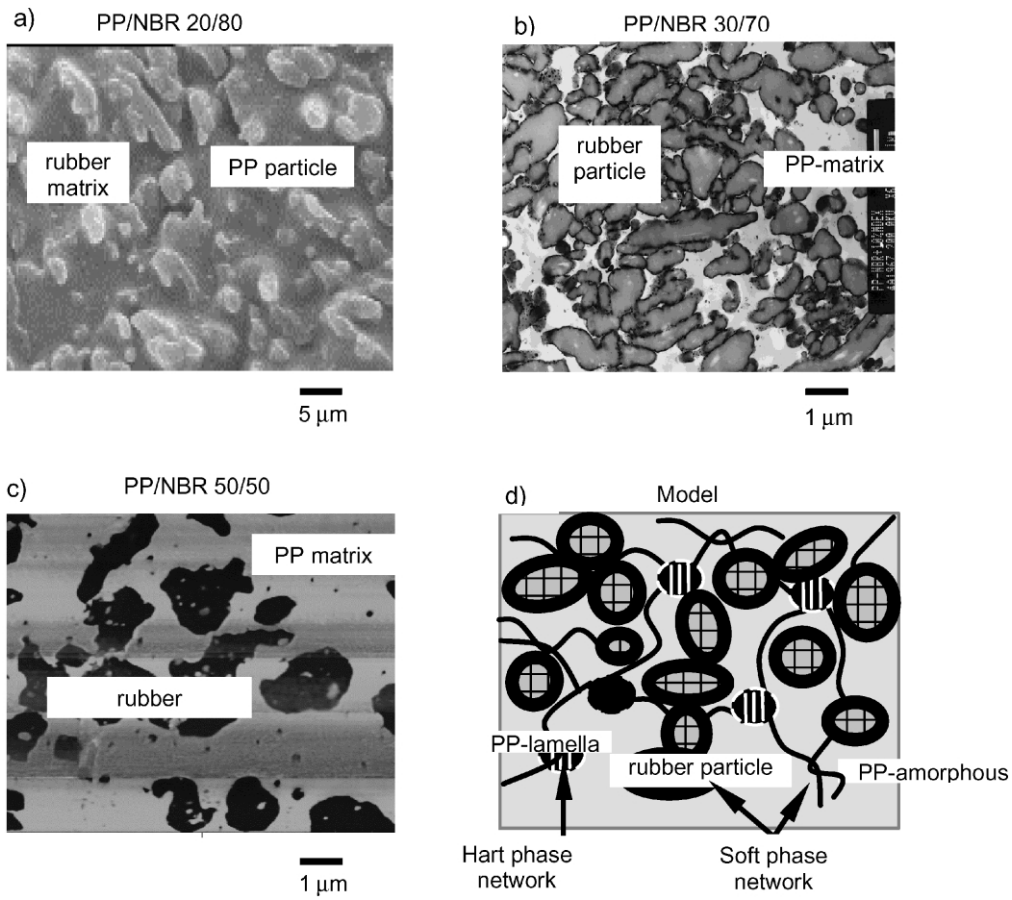

Fig. 10. Morphology of dynamic vulcanizate (a) PP/NBR 20/80 (SEM), (b) 30/70 (TEM), (c) 50/50 (AFM) and (d) the two-network model.

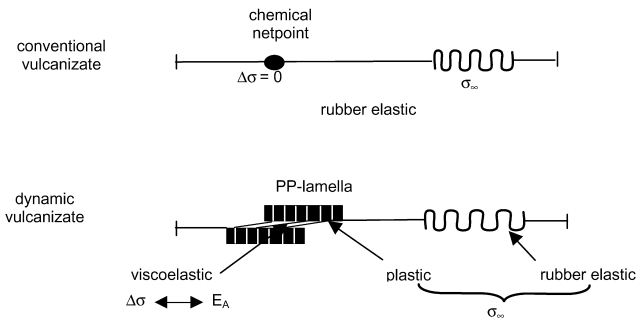

Fig. 11. Structural background of the stress components σ_∞ and $\Delta\sigma$ according to the two-network model.

3.5. Comparison with other thermoplastic elastomers

The influence of the network structure on the stress relaxation behavior can be characterized using different TPE. In Fig. 12 the morphologies of investigated TPE are shown. They were selected by having the same hardness like dynamic vulcanizate. However, the structure of the hard phase network changes stepwise away from that of dynamic vulcanizates. The ePP is an alternating block copolymer from atactic and isotactic PP blocks. ePP possesses the same crystal network like a PP-based dynamic vulcanizate. However, the elastomeric network is missing in ePP. PEBAX is also an alternating block copolymer from polyether and polyamide PA blocks. In the hard domain of PEBAX amorphous and crystalline PA phase co-exist. SEBS is a tri-block copolymer from two PS end blocks and a PEB middle block. In contrast to other TPE the hard domains in SEBS are formed only by the amorphous PS phase.

The master curves of all investigated TPE are shown in Fig. 12. In comparison to the conventional NBR-vulcanizate all TPE show a pronounced time dependence. The structural differences between TPE lead to the differences of their stress relaxation behavior. In order to clarify the influence of the network structure upon the stress relaxation behavior, the activation energy E_A and the athermal stress component σ_∞ have been investigated. In Fig. 13(a), the activation energies of the TPE are shown. The activation energy rises in the range of NBR, PEBAX, ePP, dynamic vulcanizate and SEBS. For comparison the values of the appropriate thermoplastics presenting the hard domains in the TPE are confronted on the y-axis. The good agreement between the activation energies of the TPE and the corresponding hard phases confirms that the time-dependent drop of the stress in TPE is determined considerably by the thermally activated deformation processes in the hard phase network.

In Fig. 13(b) the influence of the network structure on the temperature dependence of the athermal stress component is shown. The athermal stress component of NBR-vulcanizate remains unchanged in a broad temperature range. For different TPE however, it decreases with temperature in different manner due to different extent of the plastic deformation in the hard domains.

4. Conclusion

The analysis of the stress relaxation curves by help of the two-components model allows a consistent description as well as a structural discussion of the background of the time and temperature dependent behavior of TPE.

The influences of test conditions such as strain, strain rate and temperature can be sufficiently described by creation of a master curve. As characterizing quantities the activation energy E_A and the athermal stress component σ_∞ have been determined.

The complex stress relaxation behavior of TPE is a result of viscoelastic, elastic and plastic deformation processes. With this work it is possible to compare and assess the time-

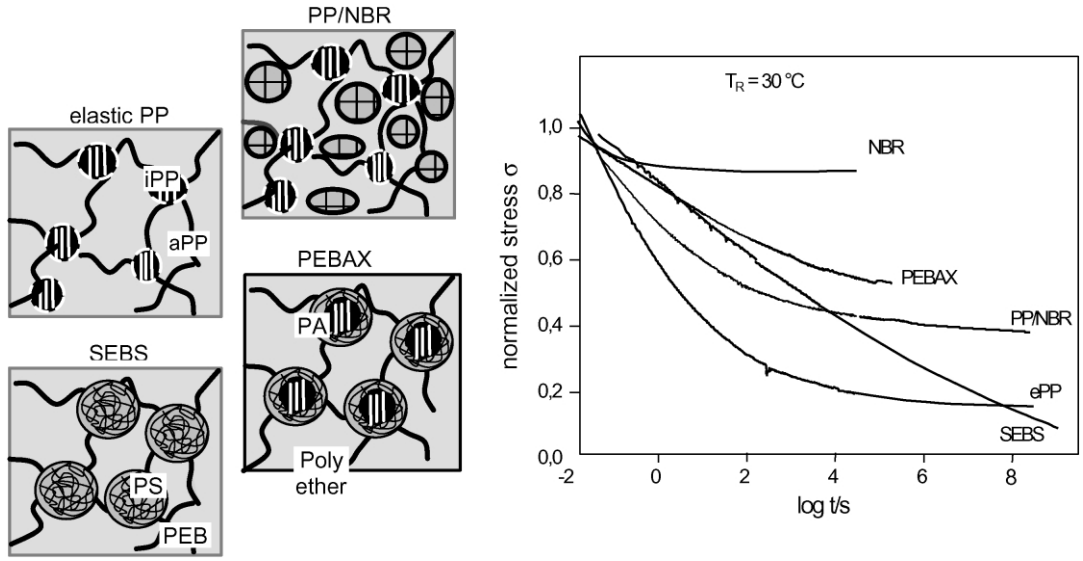

Fig. 12. Stress relaxation behavior of different TPE.

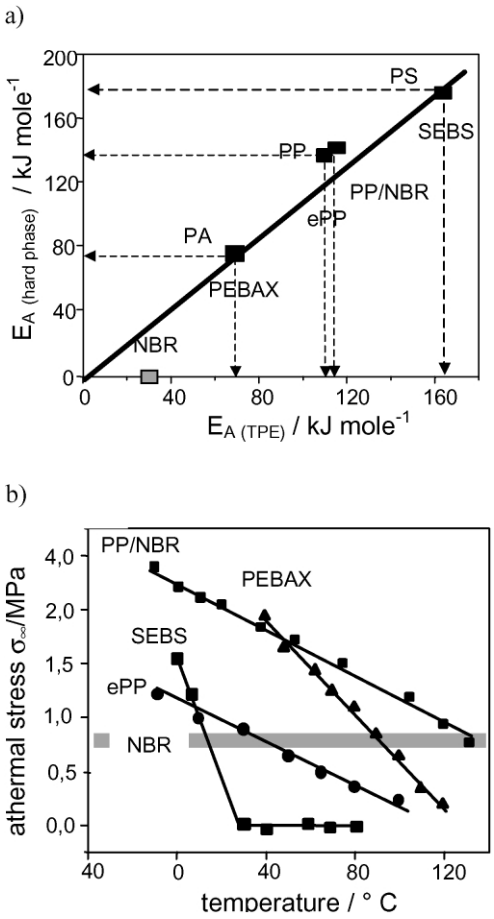

Fig. 13. Activation energy and athermal stress component of different TPE.

dependent deformation behavior of different TPE using the same evaluation procedure.

References

[1] Coran AY, Patel RP. Thermoplastic elastomers based on dynamically vulcanized elastomer–thermoplastic blends. In: Holden von G, Legge NR, Quirk R, Schroeder HE, editors. Thermoplastic elastomers. New York: Hanser/Gardner; 1996. Chapter 12.
[2] Lüpke Th, Radusch H-J. Kautsch Gummi Kunstst 1992;2:91.
[3] Lämmer E. PhD Thesis, Martin Luther University Halle-Wittenberg; 1993.
[4] Huy TA. PhD Thesis, Martin Luther University Halle-Wittenberg; 1999.
[5] Le HH. PhD Thesis, Martin Luther University Halle-Wittenberg; 2002.
[6] Corley B. PhD Thesis, Martin Luther University Halle-Wittenberg; 1999.
[7] Pham T. PhD Thesis, Martin Luther University Halle-Wittenberg; 1995.
[8] Huy TA, Le HH, Pham T, Radusch H-J. Overview of dynamic vulcanizates, POLYMERWERKSTOFFE, Halle, Germany; 21–24; September 2000.
[9] Huy TA, Lüpke Th, Radusch H-J. Kautsch Gummi Kunstst 2000;53: 656.
[10] Sengupta A, Konar BB, of J. Appl Polym Sci 1998;70:2155.
[11] Kompanient LV, Erina NA, Cheipel LM, Zelenetski AN, Prut EV. Polym Sci Ser, A 1997;39:827.
[12] Seeger A. Handbuch der Physik. Berlin: Springer; 1958.
[13] Seeger A. Z Naturforsch 1954;9a:758–856. see also p. 870.
[14] Krausz AS, Eyring H. Deformation kinetics. New York: Wiley; 1975.
[15] Ferry JD. Viscoelastic properties of polymers. New York: Wiley; 1980.
[16] Kubat J. Nature 1965;205:378.
[17] Wortmann FJ, Schulz KV. Polymer 1994;35:2108.
[18] Schulz KV, Wortmann FJ, Höcker H. Wissenschaftliche Zeitschrift TH Merseburg 1991;33:327.
[19] Wortmann FJ, Schulz KV. Polymer 1994;35:378.
[20] Wortmann FJ, Schulz KV. Polymer 1994;36:315.
[21] Wortmann FJ, Schulz KV. Polymer 1995;37:820.
[22] Wortmann FJ, Schulz KV. Polymer 1995;36:1611.
[23] Wortmann FJ. Polymer 1999;40:1611.
[24] Li JCM. Can J Phys 1967;45:493.
[25] Liu Y, Truss RW. J Polym Sci, Polym Phys Ed 1994;B32:2037.
[26] Kubat J, Seden R, Rigdahl M. Mater Sci Engng 1978;34:67.
[27] Jannas IV. J Polym Sci Macromol Rev 1974;9:163.
[28] Ilisch S, Menge H, Radusch H-J. Kautsch Gummi Kunstst 2000;53: 206.
[29] Brandrup J, Immergut EH. Polymer handbook, 3rd ed. New York: Wiley; 1989. V/29.
[30] Shapery RA. Polym Engng Sci 1969;9:295.
[31] Boyd RH. Polymer 1985;26:323.